

Finite Element Analysis on Mechanical Behaviour of Yungui Railway Tunnel in Shallow and Unsymmetrical Strata

Yang Shang-Yang^{1,2}, Li Shu-Cai¹, Xue Yi-Guo¹ and Zhang Qing-Song¹

¹. *Geotechnical & Structural Engineering Research Center, Shandong University, Jinan, 250061, China*

². *Department of Physics and Mathematics, Shandong Jiaotong University, Jinan, 250023, China*
yangsy@sdjtu.edu.cn,

Abstract

Triaxial compression tests had been performed to determine the properties of the surrounding rock. The displacement and stress of surrounding rock had been analyzed according to Silin 2 at Yungui railway under three kinds of conditions: the initial state, excavation without supporting, and supporting after excavation. Plane strain FEM was established to analyze the stability of the surrounding rock. Contrasted the monitor measuring data, the results showed that the most unfavorable position in the tunnel was found at the ridge side of the arch, and the implementation of support afforded to ensure the stability of surrounding rock, and the design of the early support approach had the ability to meet the safety requirements. The results had certain significance for understanding the mechanical behavior of shallow tunnel in unsymmetrical strata.

Keywords: *tunnel; mechanical behaviour; numerical simulation; deformation; stability*

1. Introduction

It was great necessary to simulate the excavation of tunnel using finite element program with the help of computer in tunnel engineering^{[1]-[10]}. Wang Lihong^[11] analyzed the mechanical behavior of tunnel lining using the ANSYS finite element software. The internal force of the lining and checking calculation of its carrying capacity were given in his paper. Wang Zhecao^[12] studied the deformation and stability of the underground caverns for the construction of underground crude oil storage caverns with the containment of groundwater. Silin 2 tunnel of high speed railway from Nanning to Kunming was taken as an example in this paper. Analysis and evaluation of the soft rock shallow tunnel in unsymmetrical strata were given through the establishment of plane strain finite element analysis model. Then the corresponding basis was provided for verification of the rationality of the supporting method for surrounding rock^[13].

Project situation

The tunnel analyzed in this paper was between Pingguo and Nahe in Baise city with about 40m for the biggest buried depth. New Austrian Method was used in this tunnel construction with smooth blasting and bolt-shotcrete web wet spraying method. This tunnel was belonged to V class surrounding rock and the big abut bench method was carried out in this construction. In order to strengthen the support the ring I20b steel and the small pipe were adopted. Monitoring measurement was carried out in the

基金项目：国家自然科学基金重点项目（51139004），国家自然科学基金面上项目（50979052）；教育部博士点基金（20110131110030）山东交通学院科研基金（Z201133）

作者简介：杨尚阳（1979- ），男，山东济宁人，讲师，主要从事数值计算及现场监测的研究工作。
手机：1523156602

construction organization for discrimination of stability of supporting system.

The overlying Quaternary Holocene deposits were sporadic distribution, meanwhile, the fourth section of Middle Triassic Baifeng formation shale was found everywhere underneath. Characteristics of each layer of rock and soil were as follows:

(1) The silty clay: It's common colors were brown yellow and yellowish gray. It had hard plastic and uneven structure. About 10% to 35% of the silty clay with 2 to 60 millimetre diameter consisted of shale, sandstone and rubble breccia. The silty clay was widely distributed in the period of slope surface, with the thickness of 2 ~ 5m, belonging to the class III of common soil.

(2) The shale: It's common colors were brown yellow and cinerous. It had thin layer and silty structure with highly developed foliation and general developed joints fractured. The exploration core with the shape of column or pie from fully weathered zone had the original rock structure and a small amount of breccia with the thickness of 0 ~ 2m, belonging to the class III of hard soil. The exploration core with the shape of breccia or fragment from strong weathered zone belonged to the grade IV soft stone with the thickness of 4 ~ 17m. The exploration core with the shape of chunky angle breccia or short column from weakly weathered zone belonged to the grade IV soft stone.

2. ANSYS Numerical Simulation and Analysis for the Process of Tunnel Excavation

Indoor rock triaxial test

Triaxial compression tests had been performed to determine the properties of the rock mass around Silin 2 tunnel. The sample shale was taken from the engineering site which was in 40m burial depth. The sample was cut and polished into standard one whose density was $2.0 \times 10^3 \text{ kg/m}^3$. The test equipment type RLW-500 rock triaxial apparatus was adopted (see Figure 1). According burial depth, 2MPa was used as its confining pressure.



Figure 1. RLW-500 Rock Triaxial Apparatus for the Test

According to the test results, we gained the saturated specimen block density (ρ_D), modulus of elasticity (E), poisson's ratio (ν), cohesion (c), friction angle (φ). (See Table 1)

Table 1. The Parameters of Finite Element Calculation

| category | E /GPa | ν | ρ_D kg/m^3 | C / MPa | ϕ /($^{\circ}$) |
|---------------------------|-------------|-------|----------------------|-----------------|---------------------------|
| Surrounding | 1 | 0.4 | 2000 | 0 | 27 |
| C30Reinforced concrete | 32 | 0.2 | 2500 | .4 | 50 |
| bolt | 165 | 0.3 | 8000 | - | - |

Mesh model and boundary conditions

Because the length (1500~7700 m) of the cavern was far more than its section size (20~30 m), the tunnel could be regarded as the plane strain problems to be solved. According to the actual situation of this tunnel, the numerical simulation scope was: total height of 80m, the width of 110m, and 22m buried depth. This model was divided into 3901 quadrilateral mesh units. In order to get more accurate data of the seepage and displacement field of the underground structure around the surrounding rock, the mesh intensity was increased around the tunnel. The meshing was shown in Figure 2. Stress boundary condition: horizontal restraint for model sides, vertical restraint for model bottom, free surface for model top and inner.

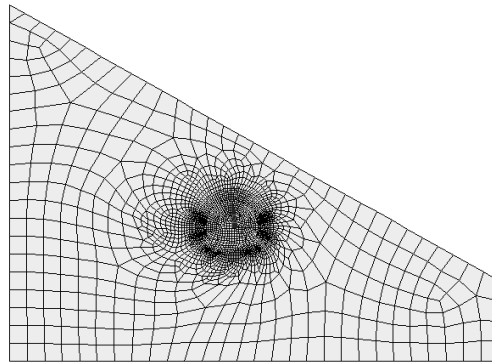


Figure 2. Mesh of the Plane Strain Model

Calculation results

Displacement field and stress field in initial state

The three states which contained the initial state before the excavation, no supporting after the excavation and with supporting after the excavation were realized by setting up three loading steps in AYSYS. The first load step which only in gravity and boundary constraint condition was set before excavation. The displacement field and stress field in initial state was shown in Figure 3.

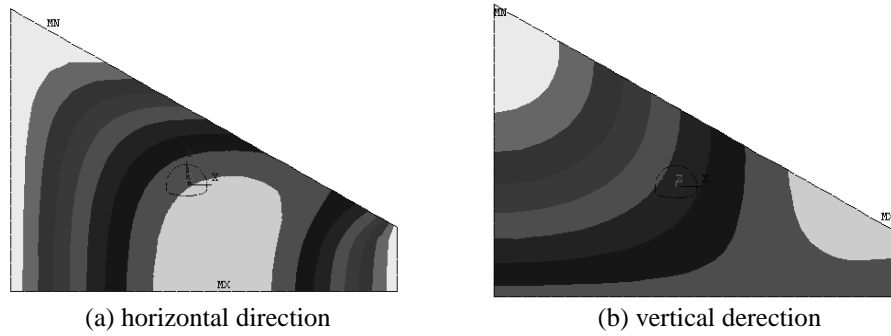


Figure 3. Displacement Contour Line Plot of Initial State / M

Because Silin 2 tunnel was in bias state, the displacement isoline was in curve distribution rather than in level before the excavation. The largest displacement in horizon was found in right-bottom, while the smallest one was found in the area near the ridges (see Figure 3). The displacement map in initial state provided reference value for the the relative displacement after excavation. The geostress-isoline was not in level in initial thus the bias characteristic of the tunnel was verified. Meanwhile, the whole calculation area in vertical direction of rock mass was in compression state, the pressure became bigger from top to down, and the maximum one was 1.13 MPa (see Figure 4).

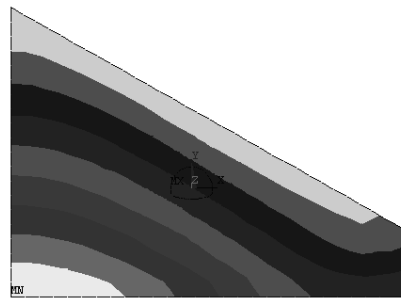


Figure 4. σ Contour Line Plot in Vertical Derection of Initial State/ Pa

Displacement field and stress field with no supporting after excavation

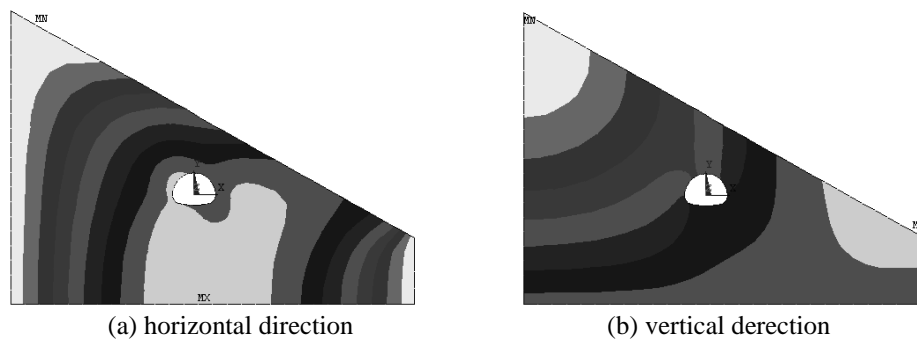


Figure 5. Displacement Contour Line Plot after Excavation without Support/ M

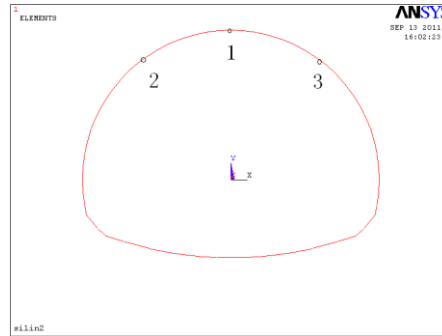


Figure 6. Distribution of Monitoring and Measuring

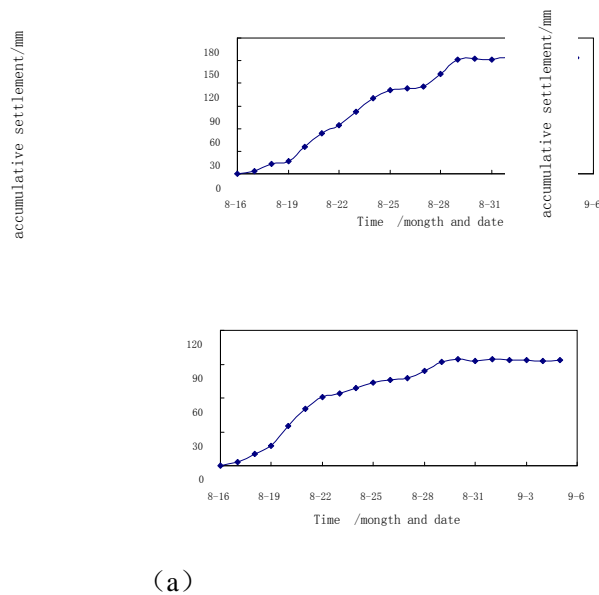


Figure 7. Vault Acumulative Settlement in Monitoring

The tunnel excavation had little effect on horizontal displacement of surrounding rock mass from the comparison Figure 5 (a) and Figure 3 (a). The displacement of the left area of vaults formed funnel-shaped distribution, and the maximum 10.12mm was found in left area of vault(see Figure 5(b)). There were three monitoring and measuring points on the vault(see Figure 6). Number 2 point represented the left vault, and number 3 point represented the right vault. Meanwhile, the vertical displacement varied greatly from the left to the right of the vault and therefore the bias characteristics of the tunnel was verified.

The monitor measuring about one section on spot was shown in Figure 7. The data of the left measuring point (number 2 point) of the vault was shown in Figure (a) of Figure 7, and the right one(number 3 point) was shown in Figure (b) of Figure 7. Compared with the calculation value using ANSYS, the monitor measuring data varied greatly. But the law of all the data was consistent with each other. All data pointed that the left vault settlement was significantly larger than in right left one. Meanwhile, the measured values of all tunnel sections measurement point were significantly greater than the calculated ones. There are three main reasons to explain the significant difference. First, the construction process of excavation, blasting and other processes, highly disturbed the rock, and the rock can easily be loose. Second, the monitoring time of the region was in the rainy season, and therefore there were obvious precipitation. Water seepage

of surrounding rock is extremely serious resulting in uneven settlement. The numerical simulation did not take into account the influence of water seepage. Third, the established model using ANSYS software was considered as a continuous medium. But the reality was very complex. The inhomogeneity was not taken into account, and therefore, it would undoubtedly bring a certain influence on the numerical simulation.

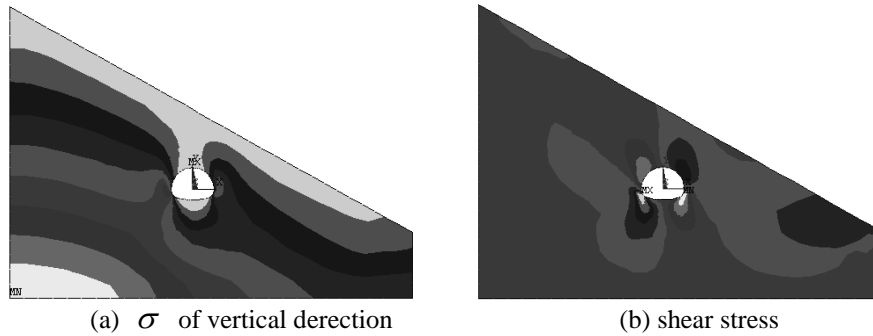


Figure 8. Stress Contour Line Plot after Excavation without Support/ Pa

After excavation, the stress redistribution was found in surrounding rock mass. The radial stress reduced but shear stress increased of the cave walls. Stress concentration was found in the cave walls. Shear stress extreme around arch feet appeared, and the extreme value was 0.3MPa(see Figure 8).

Displacement field and stress field with supporting after excavation

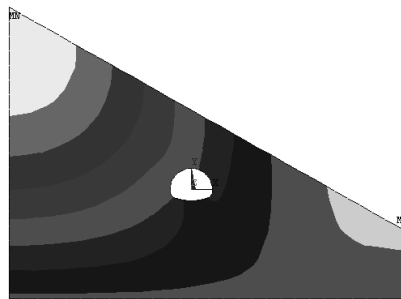


Figure 9. Vertical Displacement Contour Line Plot after Excavation with Support

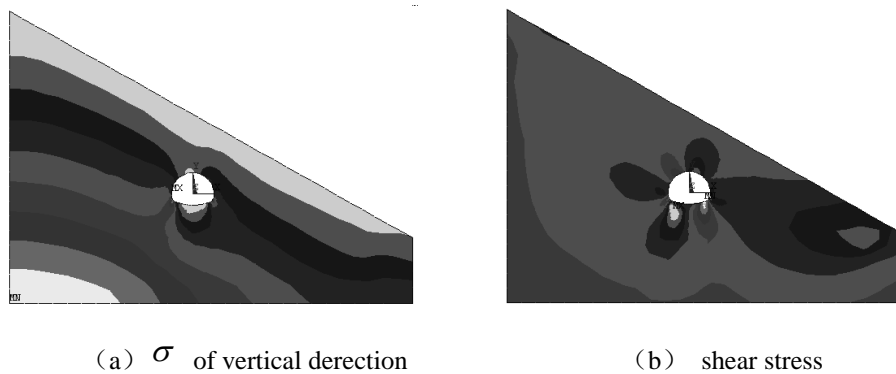


Figure 10. Stress Contour Line Plot after Excavation with Support/ Pa

Support had significant effect on the vertical displacement of surrounding rock from the comparision of Figure 5 (b) to Figure 9. After supporting, the vertical displacement isoline map of surrounding rock was no longer shown as funnel shape but similar to the

one in initial state(see Figure 3(b)). This showed that the existed supporting structure of surrounding rock played a very big role on the tunnel. Supporting had little effect on the σ of the vertical direction from comparison of Figure 10(a) and Figure 8(a). Stress concentration became weak after supporting from comparison of Figure 10(b) and Figure 8(b), with the value from 0.3 MPa to 0.2 MPa.

Internal force of beam and anchor with supporting after excavation

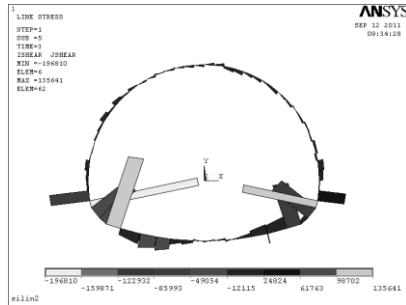


Figure 11 Shear Plot of Support Beam (Unit: N)

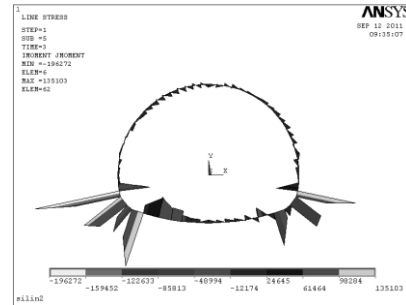


Figure 12. Bending Moment Of Beam (Unit: $N \cdot m$)

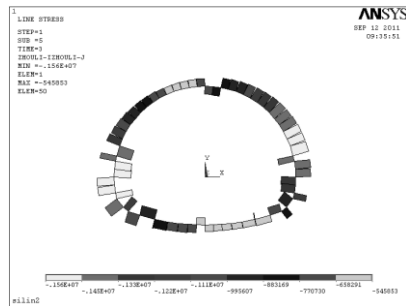


Figure 13. Axial Force Plot of Support Beam (Unit: N)

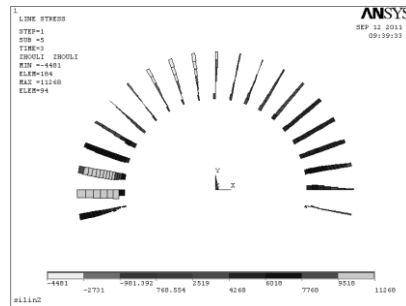


Figure 14. Axial Force Plot of Bolt (Unit: N)

In Figure 11, Figure 12 and Figure 13, whether shear or bending moment or axial force of the support beams whose maximum all appeared in the binding region of inverted arch and side wall where there was an obvious stress concentration about shear force and bending moment. The shear maximum was 196 810 N which was less than the shear strength designing value of C30 concrete. The positive bending moment maximum which appeared at the right skewback was 135 103 $N \cdot m$. The negative bending moment maximum which appeared at the left skewback was 196 272 $N \cdot m$. In Figure 14, the bolt tension maximum which appeared at the left skewback was 11 268 N . So its tensile stress was 23 MPa which was less than the allowable tensile stress of the bolt. In Figure 13, the support beam compressive stress was 5.2 MPa which was less than the compressive strength designing value of C30 concrete. The tunnel section deformation vectorgraph was shown in Figure 15. It could prove that the positive and negative bending moment maximum appeared respectively at the left skewback and the right one. In Figure 15, the tunnel laterally offset characteristic could be clearly seen. At the moment the bolt which was arranged in the left skewback had obvious tension effect. The bolt played a very big role on the stability of surrounding rock. Therefore, the bolt stress at that point needed to pay close attention to. If necessary, more bolts should be fixed up at that point to enhance the overall stability of surrounding rock.

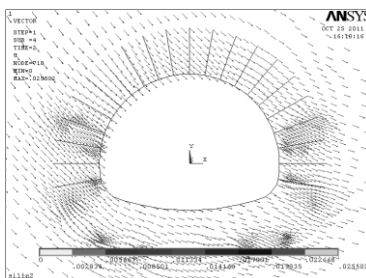


Figure 15. Vector Plot of Tunnel Deformation

3. Conclusion

Through numerical simulation of the shallow buried bias in surrounding rock tunnel construction, system understanding about the tunnel construction structure and the surrounding rock mechanics behavior was formed which was directly used to guide the construction. The existed supporting structure could effectively reduce the displacement of surrounding rock after comparison of two kinds of working conditions, and the stress concentration became significantly weak. The supporting structure in the design could guarantee the stability and security of surrounding rock.

Through the numerical simulation calculation, due to the bias tunnel, the vertical compressive stress maximum occurred at the left skewback. The support system moved towards the right hand side. Therefore, a certain number of anti-slide pile should be arranged in the left side of the tunnel before construction in case of overall shift which could make the distortion of surrounding rock and became damaged in the end. At the same time, the invert arch should be timely closed up so that the supporting structure could form an overall force.

Acknowledgement

This work was supported by the foundation under grant Monitoring and measurement of Huangdao oil reserve.

References

- [1] A. Chen, J. Gu, J. Shen, Z. Ming, L. Gu and Z. Lu, "Application study on the geomechanical model experiment techniques", Chinese Journal of Rock Mechanics and Engineering, vol. 23, no. 22, (2004), pp. 3785-3789.
- [2] S. Li, Y. Xue and Q. Zhang, "Key Technology Study On Comprehensive Prediction And Early-Warning Of Geological Hazards During Tunnel Construction In High-Risk Karst Areas", Chinese Journal of Rock Mechanics and Engineering, vol. 27, no. 7, (2008), pp. 1297-1307.
- [3] S. Li, Q. Liu and L. Li, "Development Of Large-Scale Geomechanical Model Test System For Tunnel Construction And Its Application", Chinese Journal of Rock Mechanics and Engineering, vol. 30, no. 7, (2011), pp. 1368-1374.
- [4] L. Li, S. Li, J. Chen, "Construction License Mechanism And Its Application Based On Karst Water Inrush Risk Evaluation", Chinese Journal of Rock Mechanics and Engineering, vol. 30, no. 7, (2011), pp. 1345-1355.
- [5] L. Li, "Study on catastrophe evolution mechanism of karst water inrush and its engineering application of high risk karst tunnel [Ph. D. Thesis].", Jinan: Shandong University, (2009).
- [6] D. Zhang, P. Li and Q. Fang, "Method for determining longitudinal section of subsea tunnel based on risk coefficient", Chinese Journal of Rock Mechanics and Engineering, vol. 28, no. 1, (2009), pp. 9-19.
- [7] J. Wang, P. Wang and Y. Tan, "Study on risk management of subway tunnel engineering during construction process", Chinese Journal of Underground Space and Engineering, vol. 5, no. 2, (2009), pp. 385-389.

- [8] X. Chen, B. Han and K. Liang, "Test research for surrounding rock stability of underground openings", Chinese Journal of Wuhan University of Hydraulic and Electric Engineering, (1994), vol. 27, no. 1, pp. 17–23.
- [9] Z. Li, D. Lu and H. Nakayama, "Development and application of new technology to 3D geomechanical model test of large underground houses", Chinese Journal of Rock Mechanics and Engineering, vol. 22, no. 9, (2003), pp. 1 430–1 436.
- [10] Q. Zhang, S. Li and C.'A. You, "Development and application of new type combination 3D geomechanical model test rack apparatus", Chinese Journal of Rock Mechanics and Engineering, vol. 26, no. 1, (2007), pp. 143–148.
- [11] L.-H. Wang and D.-J. Zhang, "Analysis on mechanical behavior of lining of shallow-buried and hidden excavated metro tunnel", Journal of Wuhan Institute of Technology, vol. 32, no.3, (2010), pp. 54-56.
- [12] Z.-C. Wang, S.-C. Li, Y.-G. Xue, L.-P. Qiao and C.-J. Lin, "Integrity, deformation and stability of rock mass around an underground crude oil storage caverns in containment of groundwater", Journal of Shandong University (Engineering Science), vol. 41, no. 3, (2011), pp. 112-117.
- [13] S.-Y. Yang, L.-Y. Zhang and Y. Gao, "Application of attribute recognition to highway conditions evaluation", Advanced Materials Research, (2012), pp. 2304-2308.

Authors



YANG Shang-Yang, he is a Lecturer of Department of Physics and Mathematics, Shandong Jiaotong University, Jinan, 250023, China



Li Shu-Cai, he is a Professor, Director of Geotechnical and Structural Engineering Research Center, Shandong University, Dean of Civil Engineering School, Shandong University, No.17923, Jingshi Rd., Jinan, Shandong, P.R. China.



Xue Yi-Guo, he is a Professor, teacher of Geotechnical and Structural Engineering Research Center, Shandong University, teacher of Civil Engineering School, Shandong University, No.17923, Jingshi Rd., Jinan, Shandong, P.R. China.



Zhang Qing-Song, he is a Professor, teacher of Geotechnical and Structural Engineering Research Center, Shandong University, teacher of Civil Engineering School, Shandong University, No.17923, Jingshi Rd., Jinan, Shandong, P.R. China.

